Received: 25 January 2022 | Accepted: 25 April 2022

DOI: 10.1111/jth.15745

ORIGINAL ARTICLE

$Ca_v3.2$ T-type calcium channel regulates mouse platelet activation and arterial thrombosis

Hem Kumar Tamang[1,2] | Ruey-Bing Yang[1,2] | Zong-Han Song[2] | Shao-Chun Hsu[2] | Chien-Chung Peng[3] | Yi-Chung Tung[3] | Bing-Hsiean Tzeng[4] | Chien-Chang Chen[1,2]

[1]Taiwan International Graduate Program in Molecular Medicine, National Yang Ming Chiao Tung University and Academia Sinica, Taipei, Taiwan

[2]Institute of Biomedical Sciences, Academia Sinica, Taipei, Taiwan

[3]Research Center for Applied Sciences, Academia Sinica, Taipei, Taiwan

[4]Division of Cardiology, Far Eastern Memorial Hospital and Tri-Service General Hospital, National Defense Medical Center, Taipei, Taiwan

Correspondence
Chien-Chang Chen, Institute of Biomedical Sciences, Academia Sinica, No. 128, Section 2, Academia Road, Nangang District, 115 Taipei, Taiwan.
Email: ccchen@ibms.sinica.edu.tw

Bing-Hsiean Tzeng, Cardiovascular Medical Center, Far Eastern Memorial Hospital, No. 21, Sec. 2, Nanya Rd., Banciao Dist., 220 New Taipei City, Taiwan.
Email: tzengbh@gmail.com

Funding information
This work was supported by grants from the Tri-Service General Hospital (TSGH-C104-027-002) and the Far Eastern Memorial Hospital (FEMH-2017-C-013) (B.H.T.). It was also supported by the Institute of Biomedical Sciences, Academia Sinica; MOST (102-2320-B-001-012-MY3, 105-2320-B-001-020-MY3, and 108-2320-B-001-017-MY3) (C.C.C).

Abstract

Background: $Ca_v3.2$ is a T-type calcium channel that causes low-threshold exocytosis. T-type calcium channel blockers reduce platelet granule exocytosis and aggregation. However, studies of the T-type calcium channel in platelets are lacking.

Objective: To examine the expression and role of $Ca_v3.2$ in platelet function.

Methods: Global $Ca_v3.2^{-/-}$ and platelet-specific $Ca_v3.2^{-/-}$ mice and littermate controls were used for this study. Western blot analysis was used to detect the presence of $Ca_v3.2$ and activation of the calcium-responsive protein extracellular signal-regulated kinase (ERK). Fura-2 dye was used to assess platelet calcium. Flow cytometry and light transmission aggregometry were used to evaluate platelet activation markers and aggregation, respectively. $FeCl_3$-induced thrombosis and a microfluidic flow device were used to assess *in vivo* and *ex vivo* thrombosis, respectively.

Results: $Ca_v3.2$ was expressed in mouse platelets. As compared with wild-type controls, $Ca_v3.2^{-/-}$ mouse platelets showed reduced calcium influx. Similarly, treatment with the T-type calcium channel inhibitor Ni^{2+} decreased the calcium influx in wild-type platelets. As compared with controls, both $Ca_v3.2^{-/-}$ and Ni^{2+}-treated wild-type platelets showed reduced activation of ERK. ATP release, P-selectin exposure, and $\alpha_{IIb}\beta3$ activation were reduced in $Ca_v3.2^{-/-}$ and Ni^{2+}-treated wild-type platelets, as was platelet aggregation. On *in vivo* and *ex vivo* thrombosis assay, Cav3.2 deletion caused delayed thrombus formation. However, tail bleeding assay showed intact hemostasis.

Conclusion: These results suggest that $Ca_v3.2$ is required for the optimal activation of platelets.

KEYWORDS
calcium, platelet, platelet aggregation, thrombosis, voltage-gated

Manuscript Handled by: Katsue Suzuki-Inoue

Final decision: Katsue Suzuki-Inoue, 25 April 2022

1 | INTRODUCTION

Vascular injury triggers platelet adhesion and activation, leukocyte recruitment, release of growth factors, vascular smooth muscle cell proliferation and migration, and scarring of the vessel.[1–5] Platelets play an important role in hemostasis and vessel integrity.[6,7] However, inappropriate activation of platelets causes life-threatening arterial thrombosis.[8]

During platelet activation, increased level of intracellular Ca^{2+} ($[Ca^{2+}]_i$) mediates signal transduction, which leads to platelet activation and aggregation.[9] Ca^{2+} release from internal stores and Ca^{2+} influx from the extracellular space results in increased $[Ca^{2+}]_i$ level. In addition to the known store-operated calcium entry (SOCE) and receptor-operated calcium channels, some evidence supports the possible existence of other calcium channels.[10–13] Efonidipine, a dual T- and L-type calcium channel blocker, has a strong antiplatelet effect.[10] Efonidipine improves vascular endothelial function[14] and reduces activation markers in platelets and monocytes in hypertensive patients.[10]

T-type calcium channels are voltage-gated calcium channels that activate at lower membrane potentials (approximately −70 to −60 mV) and mediate transient calcium currents. $Ca_v3.1$, $Ca_v3.2$, and $Ca_v3.3$ are the three different isoforms present in mammals.[15,16] Although predominantly expressed in excitable cells,[17] $Ca_v3.1$ and $Ca_v3.2$ are found in several nonexcitable cells.[18–21] T-type calcium channels exert their function tissue-specifically. $Ca_v3.2$ mediates exocytosis in rat chromaffin cells,[22,23] cardiac hypertrophy in response to pressure overload,[24] and tracheal chondrogenesis.[25] Similarly, $Ca_v3.1$ regulates vascular smooth muscle cell proliferation during neointimal formation[26] and calcium-dependent von Willebrand factor release from lung endothelial cells.[27] Antiplatelet activity of T-type calcium channel blockers[10] and evidence of T-type calcium channel-mediated exocytosis in nonexcitable cells indicates the possibility of involvement of these calcium channels in platelets.[18,27] However, study of the presence and role of T-type calcium channels in platelets is lacking.

The current study focused on the role of the $Ca_v3.2$ T-type calcium channel in platelet activity and arterial thrombosis. $Ca_v3.2$ is a transmembrane calcium channel. Therefore, we investigated the effect of $Ca_v3.2$ deletion and treatment with Ni^{2+} (an inhibitor of the $Ca_v3.2$ T-type calcium channel) in the change in $[Ca^{2+}]_i$ level in platelets and downstream extracellular signal-regulated kinase (ERK) activation. Calcium-activated ERK is associated with platelet granule release and integrin activation, so we assessed platelet granule release by measuring adenosine triphosphate (ATP) release, P-selectin exposure and $\alpha_{IIb}\beta3$ integrin activation. We further used a platelet functional study, measuring platelet aggregation of $Ca_v3.2^{-/-}$ and Ni^{2+}-treated platelets. Next, we used $FeCl_3$-induced thrombosis to study arterial thrombosis in mice with knockout of $Ca_v3.2$ (global and platelet-specific). This model mimics the endothelial damage and extracellular matrix exposure that mediates thrombus formation. To further consolidate our *in vivo* thrombosis findings, we used an *ex vivo* thrombosis assay with a microfluidic flow chamber device that simulates the blood flow, vessel wall injury, and thrombus growth.

Essentials

- $Ca_v3.2$ is a T-type calcium channel that activates at low voltage. It is expressed in excitatory and non-excitatory cells. $Ca_v3.2$ mediates low-threshold exocytosis.
- We studied the expression and role of $Ca_v3.2$ in platelet function in a mouse model.
- $Ca_v3.2$ was expressed in mouse platelets and was responsible for calcium influx and calcium-mediated platelet activity.
- $Ca_v3.2$ may regulate arterial thrombosis in mice.

2 | METHODS

2.1 | Mice

All conducted research conformed to the appropriate US National Institutes of Health guidelines and those of the Institutional Animal Care and Utilization Committee, Academia Sinica and Far Eastern Memorial Hospital (Taipei). Adult male and female C57BL/6J mice 8–16 weeks old were used as controls. Global $Ca_v3.2^{-/-}$ mice were generated as described.[28] To generate platelet-specific $Ca_v3.2$ conditional knockout ($Ca_v3.2^{plt-/-}$) mice, we crossbred platelet factor 4 ($pf4^{cre/+}$)[29,30] and $Ca_v3.2^{fl/fl}$ mice (detailed methods for generating flox mice are described in Supplementary Materials). Mice with the genotype $pf4^{cre/+}$; $Ca_v3.2^{fl/fl}$ were defined as $Ca_v3.2^{plt-/-}$ mice and those with the genotype $pf4^{+/+}$; $Ca_v3.2^{fl/fl}$ were littermate controls. We used C57BL/6J wild-type control mice that were age- and sex-matched to global $Ca_v3.2^{-/-}$ mice and $Ca_v3.2^{fl/fl}$ mice matched to platelet-specific $Ca_v3.2^{-/-}$ mice ($Ca_v3.2^{plt-/-}$). The primer sets (1+2; forward: 5′-aataccagcctatgtcctgt-3′ and reverse: 5′-gtataactggagggacatgg-3′) and (1+4; forward: 5′-aataccagcctatgtcctgt-3′ and reverse: 5′-cctgagacatggatgtttgg-3′) were used for G protein-coupled receptor to confirm the $Ca_v3.2^{fl/fl}$ and $Ca_v3.2$ ($pf4^{cre/+}$; $Ca_v3.2^{fl/fl}$) conditional knockout.

2.2 | Measurement of intracellular calcium ($[Ca^{2+}]_i$)

Fura-2 (10 μM) was added to 7.5×10^8 cells/ml platelets in Tyrode's albumin buffer and incubated at 37˚C for 40 min. The platelets were then washed three times. Finally, fura-2-loaded platelets were adjusted to 7×10^7 cells/ml and $CaCl_2$ (2 mM) was added as required. For global calcium concentration studies, thrombin and calcium were added together, and for calcium influx study, calcium was added 2 min after thrombin stimulation. For adenosine diphosphate (ADP)-induced rescue studies, ADP (0.02 μM) was added immediately after the addition of thrombin. Platelets were activated with thrombin/ADP, then Triton X-100 (0.1%) and EGTA (8 mM), and fluorescence intensity was measured by spectrofluorometry (FP8500, JASCO). The platelet $[Ca^{2+}]_i$ level was calculated as described.[31] The following formula was used to calculate calcium concentration: $[Ca^{2+}]_i = K_D\ X[(R\text{-}R_{min})/(R_{max}\text{ -}R)]X(Sf_2/Sb_2)$, where K_D =

the dissociation constant of the dye for Ca^{2+} at the chosen experimental condition (K_D =224 nM at our experimental conditions); R = the ratio of the fluorescence intensities at the two wavelengths (340/380); R_{min} = the ratio value obtained after the addition of EGTA 8 mM; R_{max} = the ratio value obtained after the addition of Triton X-100 0.1%; Sf_2 = the maximum fluorescence intensity obtained at 380 nM; and Sb_2 = the minimum fluorescence intensity obtained at 380 nM.

2.3 | Western blot analysis

Western blot analysis was performed as described.[32] In brief, platelets were activated with agonists at 37°C in an aggregometer, and an equal volume of ice-cold 2X lysis buffer (Tris/HCl 100 mM, pH 7.4, NaCl 400 mM, $MgCl_2$ 5 mM, Nonidet P-40 2%, glycerol 20%, and complete protease inhibitor cocktail lacking EDTA) was added after 3 min. Protein lysates were run through the sodium dodecyl sulfate–polyacrylamide gel electrophoresis, then transferred onto PVDF membranes. The proteins were probed with phosphorylated ERK (pERK), tERK, and β-actin antibodies. Western blot images were taken by using LAS-4000 mini (Fujifilm) and images were analyzed and quantified by using ImageJ.

We transiently expressed $Ca_v3.2$ (human and mouse clone) and $Ca_v3.1$ (human clone) in HEK 293 cells. We used total protein lysates of these cells for control experiments and the membrane protein-enriched fraction of mouse platelets and testes for sodium dodecyl sulfate–polyacrylamide gel electrophoresis. Proteins were transferred to PVDF membranes and anti-$Ca_v3.2$ antibody C1868 (Sigma) was used to detect signals.

2.4 | Electron microscopy

Platelets were fixed with glutaraldehyde (2.5%) in a phosphate buffer (0.1 M, pH 7.4) for 1 h at room temperature. After fixation, the sample was washed three times with phosphate buffer and processed as described.[33] Images were obtained by using a transmission electron microscope (FEI Tecnai G2 F20 S-TWIN).

2.5 | Statistical analysis

Statistical analysis was performed with Sigmaplot and GraphPad Prism 6. Unpaired Student *t*-tests, Mann-Whitney *U* test (nonparametric), one-way repeated measures analysis of variance (ANOVA) with Holm-Sidak post hoc test or one-way ANOVA with Tukey post hoc test were used to assess statistical significance. For all experiments, $p < .05$ was considered statistically significant.

Additional methods and materials are in Supplementary files.

2.6 | Data sharing statement

For original data, please contact Chien-Change Chen at ccchen@ibms.sinica.edu.tw.

3 | RESULTS

3.1 | Expression of $Ca_v3.2$ T type calcium channel in mouse platelets

Our reverse transcriptase-polymerase chain reaction results from CD41-positive cells (megakaryocytes) demonstrated that $Ca_v3.2$ was expressed in mouse megakaryocytes (Figure 1A). To further confirm the expression of $Ca_v3.2$ in platelets, we used western blot analysis. We tested several commercially available antibodies to detect $Ca_v3.2$ in platelets and finally chose anti-$Ca_v3.2$ antibody C1868 (Sigma) for our experiments. We first tested the specificity of the antibodies by

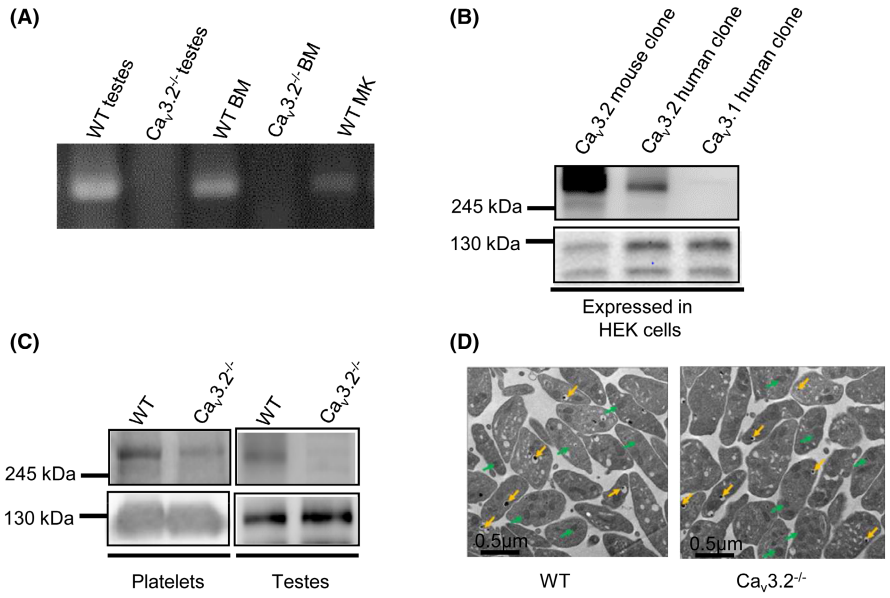

FIGURE 1 Expression of $Ca_v3.2$ T-type calcium channel in mouse platelets. (A) Detection of $Ca_v3.2$ mRNA expression by reverse transcriptase-polymerase chain reaction. BM, bone marrow; MK, megakaryocytes; WT, wild-type. (B) Detection of human and mouse clones of $Ca_v3.2$ expressed in HEK 293 cells. (C) Detection of $Ca_v3.2$ in mouse platelets and testes. (D) Transmission electron microscopy of platelets. The yellow arrows show the dense granules and the green arrows the alpha granules. Scale bar = 0.5 μm.

using $Ca_v3.2$ or $Ca_v3.1$ transiently expressed in HEK 293 cells. The antibody could detect $Ca_v3.2$ but not $Ca_v3.1$ expressed in HEK 293 cells (Figure 1B). Similarly, $Ca_v3.2$ could be detected in wild-type mouse platelets and testes but not in $Ca_v3.2^{-/-}$ controls (Figure 1C).

Next, we performed a complete blood cell count. $Ca_v3.2^{-/-}$ or $Ca_v3.2^{plt-/-}$ (global or platelet specific) mice and controls (Table 1) did not differ in counts. Similarly, we found no significant difference in granulation or morphology in $Ca_v3.2^{-/-}$ platelets (Figure 1D).

3.2 | Activation-induced change in $[Ca^{2+}]_i$ level was decreased in $Ca_v3.2^{-/-}$ and Ni^{2+}-treated platelets

Stimulation elevates $[Ca^{2+}]_i$ level in platelets.[9] To study the role of $Ca_v3.2$ in change in platelet $[Ca^{2+}]_i$ concentration, we used fura-2-loaded platelets to assess the global $[Ca^{2+}]_i$ concentration, calcium release from internal stores and calcium entry. $Ca_v3.2^{-/-}$ platelets showed reduced global change in calcium concentration in response to thrombin (451 ± 15 nM for $Ca_v3.2^{-/-}$ vs. 530 ± 12 nM for controls, $p = .015$; Figure 2A). All calcium concentration values stated are peak values.

To differentiate between calcium release or calcium entry defects, we activated platelets in the presence of EGTA (1 mM) for 2 min to induce calcium release from internal stores, then $CaCl_2$ (2 mM) was added to induce calcium influx. The calcium release from internal stores was minimal but similar in both $Ca_v3.2^{-/-}$ and wild-type platelets. However, $Ca_v3.2^{-/-}$ platelets showed decreased calcium influx after the addition of $CaCl_2$ (2 mM) (431 ± 13 nM for $Ca_v3.2^{-/-}$ vs. 499 ± 17 nM for controls, $p = .01$; Figure 2B). To rule out the effect of released ATP and ADP, calcium influx was measured in the presence of apyrase (5 U/ml). The findings confirm that the calcium influx defect in $Ca_v3.2^{-/-}$ platelets (443.3 ± 10.9 nM for $Ca_v3.2^{-/-}$ vs. 513 ± 14.2 nM for controls, $p = .02$; Figure 2C) was independent of ADP release.

Store-operated calcium entry is important for elevating $[Ca^{2+}]_i$ level.[9] To evaluate SOCE, we assessed calcium influx induced by thapsigargin (100 nM). Calcium influx mediated by thapsigargin was comparable in $Ca_v3.2^{-/-}$ and wild-type controls (931.2 ± 50.8 vs. 897 ± 53.1, $p = .9$; Figure S1A). Thus, calcium influx defect in $Ca_v3.2^{-/-}$ platelets was not attributed to SOCE.

Ni^{2+} at low concentrations specifically inhibits $Ca_v3.2$.[22,34,35] We used $NiCl_2$ to assess the effect of Ni^{2+} on change in platelet $[Ca^{2+}]_i$ level. Ni^{2+} treatment (30 μM) reduced the global calcium concentration in response to thrombin (325 ± 16.5 for Ni^{2+}-treated platelets vs. 397.7 ± 14.6 for vehicle controls, $p = .002$; Figure 2D). Similarly, calcium influx but not calcium release was reduced in Ni^{2+}-treated platelets (280.1 ± 10.7 nM for Ni^{2+}-treated platelets vs. 337.5 ± 19 nM for vehicle controls, $p = .01$; Figure 2E). Ni^{2+} reduced both global calcium concentration and calcium influx. Decreased calcium influx induced by Ni^{2+} was not affected by apyrase (224.9 ± 31.3 nM for Ni2+-treated platelets vs. 266.2 ± 24.8 nM for vehicle control, $p = .04$; Figure 2F). Ni^{2+} treatment had no effect on calcium influx mediated by thapsigargin in wild-type platelets (Figure S1B). These results suggest that $Ca_v3.2$ plays a role in calcium influx.

3.3 | Deletion of $Ca_v3.2$ or application of its inhibitor (Ni^{2+}) reduced phosphorylation of ERK in platelets during activation

Calcium-mediated phosphorylation of ERK mediates platelet activity.[32,36,37] Moreover, $Ca_v3.2$-dependent activation of ERK in the

	WT	$Ca_v3.2^{-/-}$	$Ca_v3.2^{fl/fl}$	$Ca_v3.2^{plt-/-}$
Hb (g/dl)	15.01 ± 0.18	14.27 ± 0.34	15.92 ± 0.33	14.5 ± 0.53
WBC count (10^3/μl)	8.97 ± 1.00	9.4 ± 1.03	9.58 ± 0.94	9.93 ± 0.72
RBC count (10^3/μl)	9.82 ± 0.18	9.06 ± 0.23	9.97 ± 0.25	9.77 ± 0.37
Hematocrit (%)	50.6 ± 0.79	47.2 ± 1.17	48.44 ± 1.81	51.2 ± 1.87
Platelet count (10^3/μl)	819 ± 60.62	760.28 ± 64.54	725.8 ± 38.6	768.2 ± 46.9
MPV (fL)	7.54 ± 0.22	7.60 ± 0.21	7.14 ± 0.04	7.42 ± 0.03

Note: An automated hematology cell counter was used for complete blood cell counts.
Data are mean ± SEM.
$N = 7$ (WT and $Ca_v3.2^{-/-}$) and $N = 5$ ($Ca_v3.2^{fl/fl}$ and $Ca_v3.2^{plt-/-}$).
Hematologic parameter values did not significantly differ among the four groups.
Hb, hemoglobin; MPV, mean platelet volume; RBC, red blood cell; WBC, white blood cell.

TABLE 1 Complete blood cell counts in circulation for wild-type (WT), $Ca_v3.2^{-/-}$, $Ca_v3.2^{fl/fl}$, and $Ca_v3.2^{plt-/-}$ mice

FIGURE 2 Intracellular calcium concentration is reduced during activation of $Ca_v3.2^{-/-}$ and Ni^{2+}-treated platelets. (A) Change in global calcium content in WT and $Ca_v3.2^{-/-}$ platelets ($p = .015$, wild-type [WT] vs. $Ca_v3.2^{-/-}$). (B) Calcium mobilization within the first 2 min with no calcium between $Ca_v3.2^{-/-}$ and WT platelets. Calcium influx initiated after the addition of calcium (2 mM) in $Ca_v3.2^{-/-}$ platelets versus WT controls (*$p = .01$, WT vs. $Ca_v3.2^{-/-}$). (C) Calcium influx mediated by thrombin 10 mU/ml in the presence of apyrase 5 U/ml ($p = .002$, WT vs. $Ca_v3.2^{-/-}$). (D) Change in global calcium content and (E) calcium influx in Ni^{2+}-treated platelets ($p = .002$, for global calcium concentration; *$p = .01$, for calcium influx, vehicle vs. Ni^{2+}). (F) Calcium influx mediated by thrombin 10 mU/ml in the presence of apyrase 5 U/ml (*$p = .04$, Veh vs. Ni^{2+}-treated platelets). Data are mean ± SEM ($N = 3$–5) and were analyzed by unpaired *t*-test with Mann-Whitney *U* test and ANOVA with Tukey's multiple comparison test. ANOVA, analysis of variance; veh, vehicle.

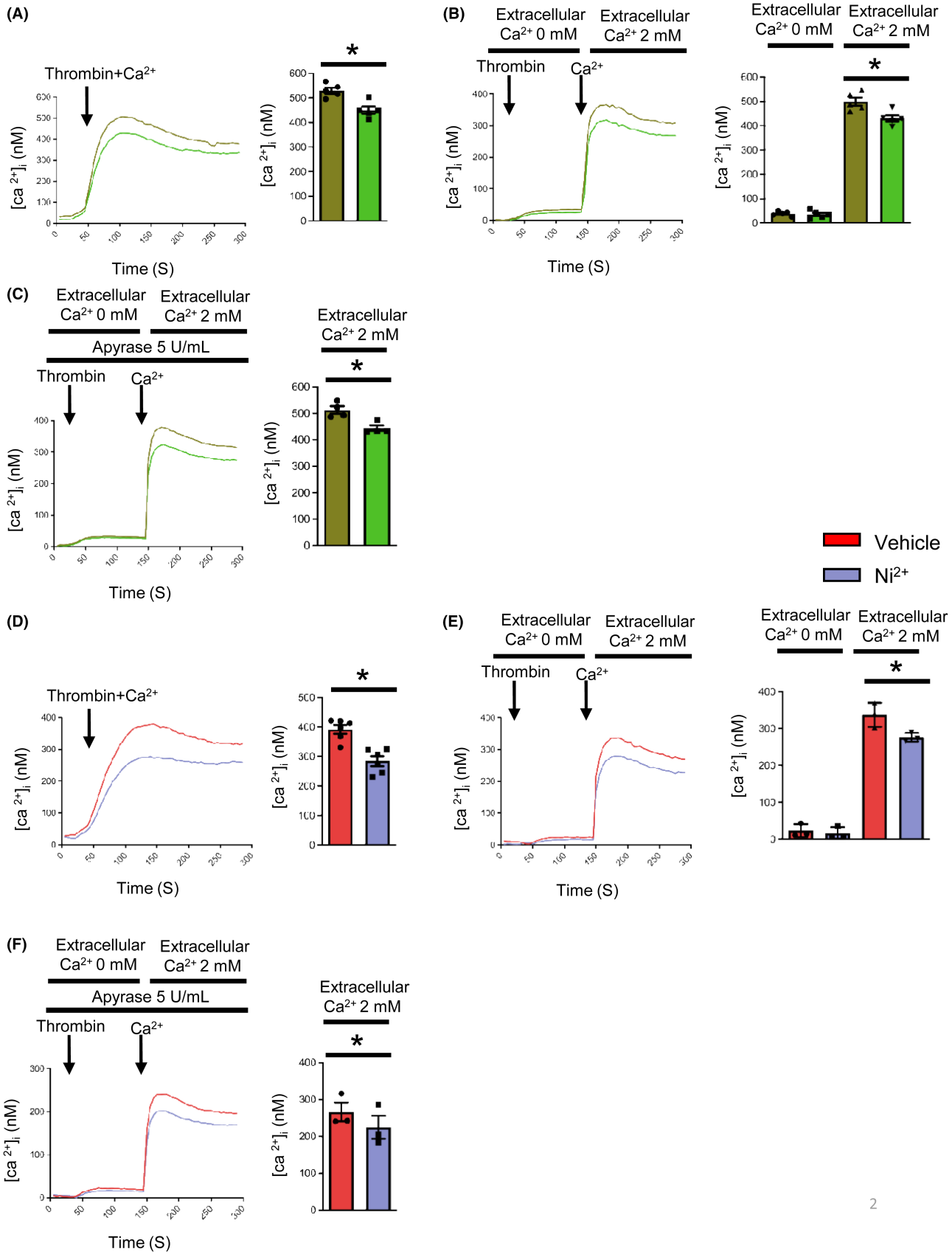
WT
Cav3.2-/-
(A)
Thrombin+Ca2+
[ca 2+]i (nM)
Time (S)
(B)
Extracellular Ca2+ 0 mM
Extracellular Ca2+ 2 mM
Thrombin
Ca2+
(C)
Apyrase 5 U/mL
Vehicle
Ni2+
(D)
(E)
(F)

paraventricular thalamus regulates chronic pain.[38] Our western blot results demonstrated that ERK phosphorylation induced by thrombin was significantly reduced in $Ca_v3.2^{-/-}$ platelets ($p = .01$; Figure 3A,B).

Similarly, ERK phosphorylation was significantly reduced in Ni^{2+}-treated platelets ($p = .04$; Figure 3C,D). Ni^{2+} did not further decrease the pERK level in $Ca_v3.2^{-/-}$ platelets (Figure 3E,F). Thus, deletion of $Ca_v3.2$ or its inhibitor reduced ERK activation.

3.4 | Granule secretion and activation of integrin $\alpha_{IIb}\beta3$ is impaired in $Ca_v3.2^{-/-}$ platelets

Calcium mediates platelet secretion and $\alpha_{IIb}\beta3$ activation via ERK activation.[32] ATP release induced by collagen (62.7 ± 8.5 picomole/10^7 cells for $Ca_v3.2^{-/-}$ vs. 94.4 ± 5.9 picomole/10^7 cells for controls, $p = .02$; Figure 4A) or thrombin (67.9 ± 11.1 vs. 97.5 ± 10.2 picomoles/10^7 cells, $p = .04$; Figure 4B) from $Ca_v3.2^{-/-}$ platelets was significantly reduced.

Defective ATP release could be due to less ATP being available for release or less ATP in $Ca_v3.2^{-/-}$ platelets. Therefore, we assessed the amount of releasable ATP and total ATP content in platelets. In response to thrombin (2 U/ml), ATP released from $Ca_v3.2^{-/-}$ platelets was similar to that in wild-type controls (737.8 ± 40 nM vs. 796.4 ± 70.3 nM, $p = .5$; Figure S2A). Similarly, total ATP content in $Ca_v3.2^{-/-}$ and control platelets was comparable (57.3 ± 5.9 nM vs. 61.3 ± 5.9 nM, $p = .8$; Figure S2B).

$Ca_v3.2^{-/-}$ platelets showed significantly reduced P-selectin exposure compared with controls (1058 ± 102.2 mean fluorescence

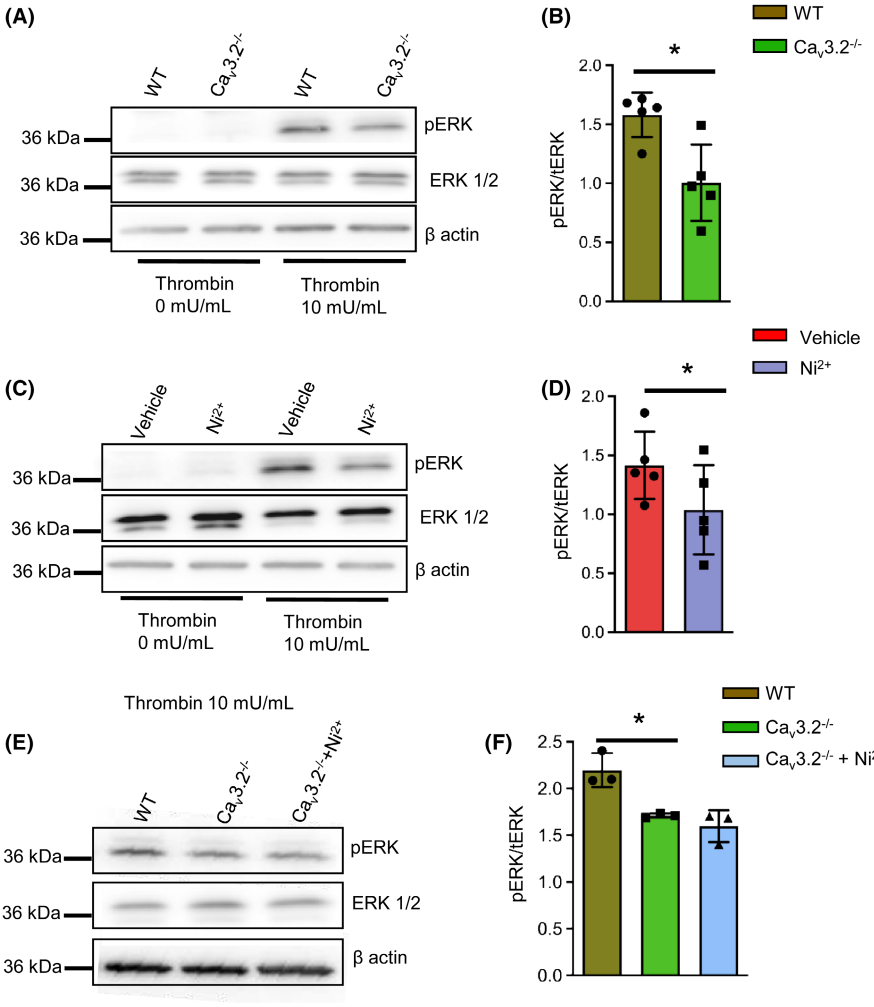

FIGURE 3 ERK activation is reduced in $Ca_v3.2^{-/-}$ and Ni^{2+}-treated platelets. (A) Representative western blot image showing reduced pERK level in $Ca_v3.2^{-/-}$ platelets activated with thrombin (10 mU/ml). (B) Quantification of pERK/tERK ratio (*$p = .01$, WT vs. $Ca_v3.2^{-/-}$). (C) Representative western blot image showing reduced pERK level in Ni^{2+}-treated WT platelets activated with thrombin (10 mU/ml). (D) Quantification of pERK/tERK ratio, (*$p = .04$, vehicle vs. Ni^{2+}). (E) Thrombin-induced ERK activation; comparison between WT, $Ca_v3.2^{-/-}$ and Ni^{2+}-treated $Ca_v3.2^{-/-}$ platelets. (F) Quantification of pERK/tERK ratio. Data are mean ± SEM ($N = 3–5$) and were analyzed by paired and unpaired *t*-test and ANOVA with Tukey's multiple comparison test. ANOVA, analysis of variance.

FIGURE 4 Granule release and integrin $\alpha_{IIb}\beta3$ activation are reduced in $Ca_v3.2^{-/-}$ and Ni^{2+}-treated platelets. ATP release induced by (A) collagen (0.8 μg/ml) and (B) thrombin (10 mU/ml) ($n = 3–5$, *$p = .02$, WT vs. $Ca_v3.2^{-/-}$ platelets activated with collagen 0.8 μg/ml; $n = 4–5$, *$p = .04$, with thrombin 10 mU/ml). Detection of P-selectin (C) or activated integrin $\alpha_{IIb}\beta3$ (D) by flow cytometry and activated with thrombin (10 mU/ml). Data are mean fluorescence intensity (MFI) and were analyzed by one-way ANOVA followed by Tukey's multiple comparison test; ($n = 3–5$, *$p = .03$, WT vs. $Ca_v3.2^{-/-}$ for P-selectin; $n = 4–5$, *$p = .001$, for activated integrin $\alpha_{IIb}\beta3$). (E–G) Platelet granule release and integrin αIIbβ3 activation mediated by thrombin 10 mU/ml. (E) ATP release (*$p = .03$, vehicle vs. Ni^{2+}), (F) P-selectin exposure (*$p = .001$, vehicle vs. Ni^{2+}) and (G) activated $\alpha_{IIb}\beta3$ (*$p = .01$, vehicle vs. Ni^{2+}) in Ni^{2+}-treated platelets. Data are mean ± SEM and were analyzed by one-way ANOVA followed by Tukey's multiple comparison test. ANOVA, analysis of variance.

intensity [MFI] vs. 1306.6 ± 107.3 MFI, $p = .001$; Figure 4C). Activated $\alpha_{IIb}\beta3$ amplifies activation signals and platelet aggregation.[39] Similarly, $\alpha_{IIb}\beta3$ activation was significantly reduced in $Ca_v3.2^{-/-}$ versus control platelets (1991.5 ± 214.6 MFI vs. 2876 ± 234.8 MFI, $p = .001$; Figure 4D). The expression of integrin and platelet receptors was intact in $Ca_v3.2^{-/-}$ platelets (Figure S3). These findings suggest that $Ca_v3.2^{-/-}$ platelets have granule-release and $\alpha_{IIb}\beta3$-activation defects.

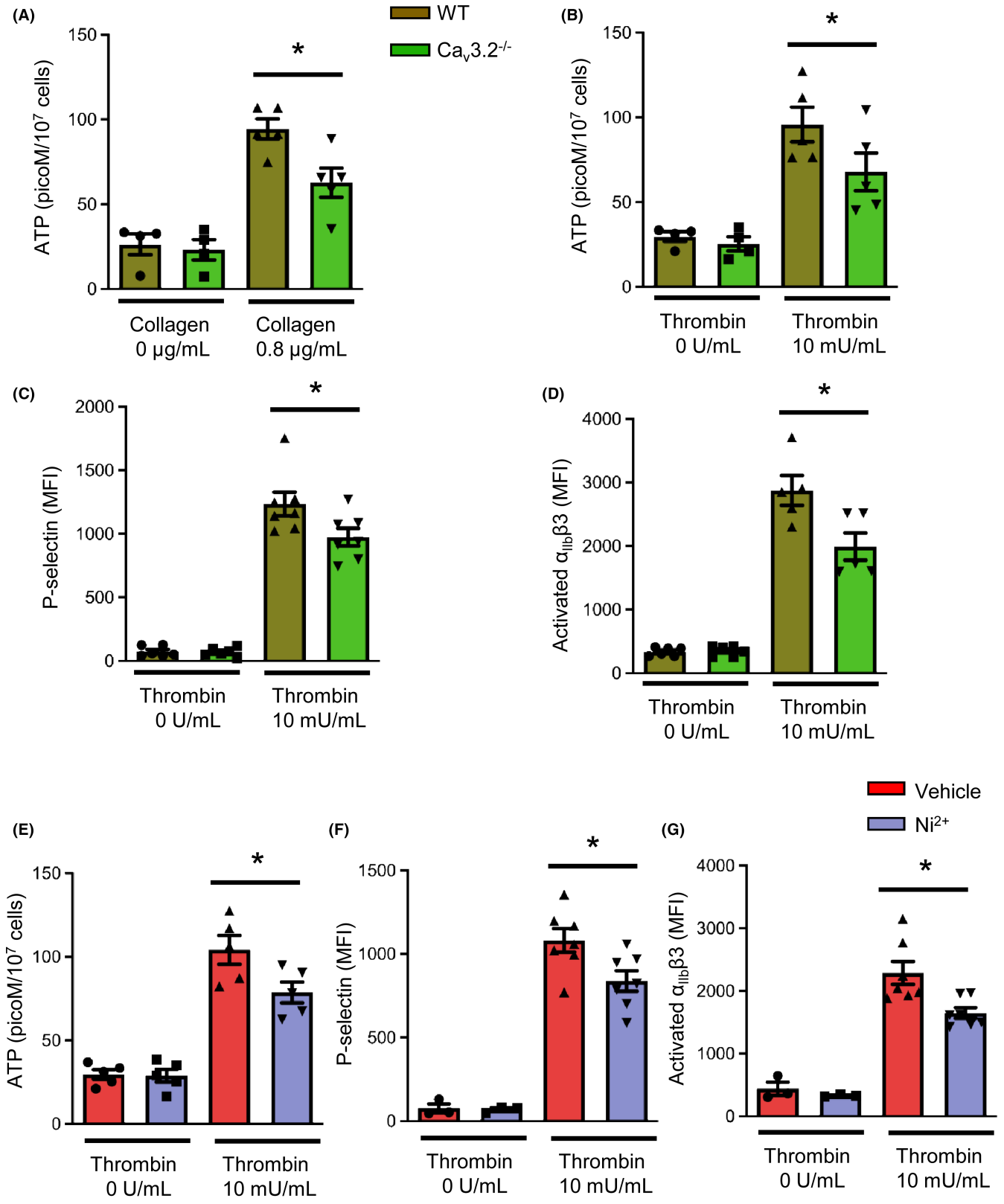

Similarly, Ni^{2+} significantly decreased ATP release in $Ca_v3.2^{-/-}$ versus control platelets (79.7 ± 5.6 picomole/10^7 cells vs. 104.1 ± 8.6 picomole/10^7 cells, $p = .03$; Figure 4E) as well as P-selectin exposure (838.6 ± 62.3 vs. 1081.6 ± 69.8 MFI, $p = .001$; Figure 4F). Ni^{2+} also reduced the activation of integrin $\alpha_{IIb}\beta3$ in $Ca_v3.2^{-/-}$ versus control platelets (1650.9 ± 84.9 MFI vs. 2287.6 ± 184.1 MFI, $p = .01$; Figure 4G). We treated $Ca_v3.2^{-/-}$ platelets with Ni^{2+} (30 μM) to investigate whether Ni^{2+} can induce a further reduction in the secretion of $Ca_v3.2^{-/-}$ platelets. As expected, Ni^{2+} had a minimal effect on ATP release from $Ca_v3.2^{-/-}$ platelets (Figure S4). Our results suggest that $Ca_v3.2$ regulates platelet granule secretion and activation.

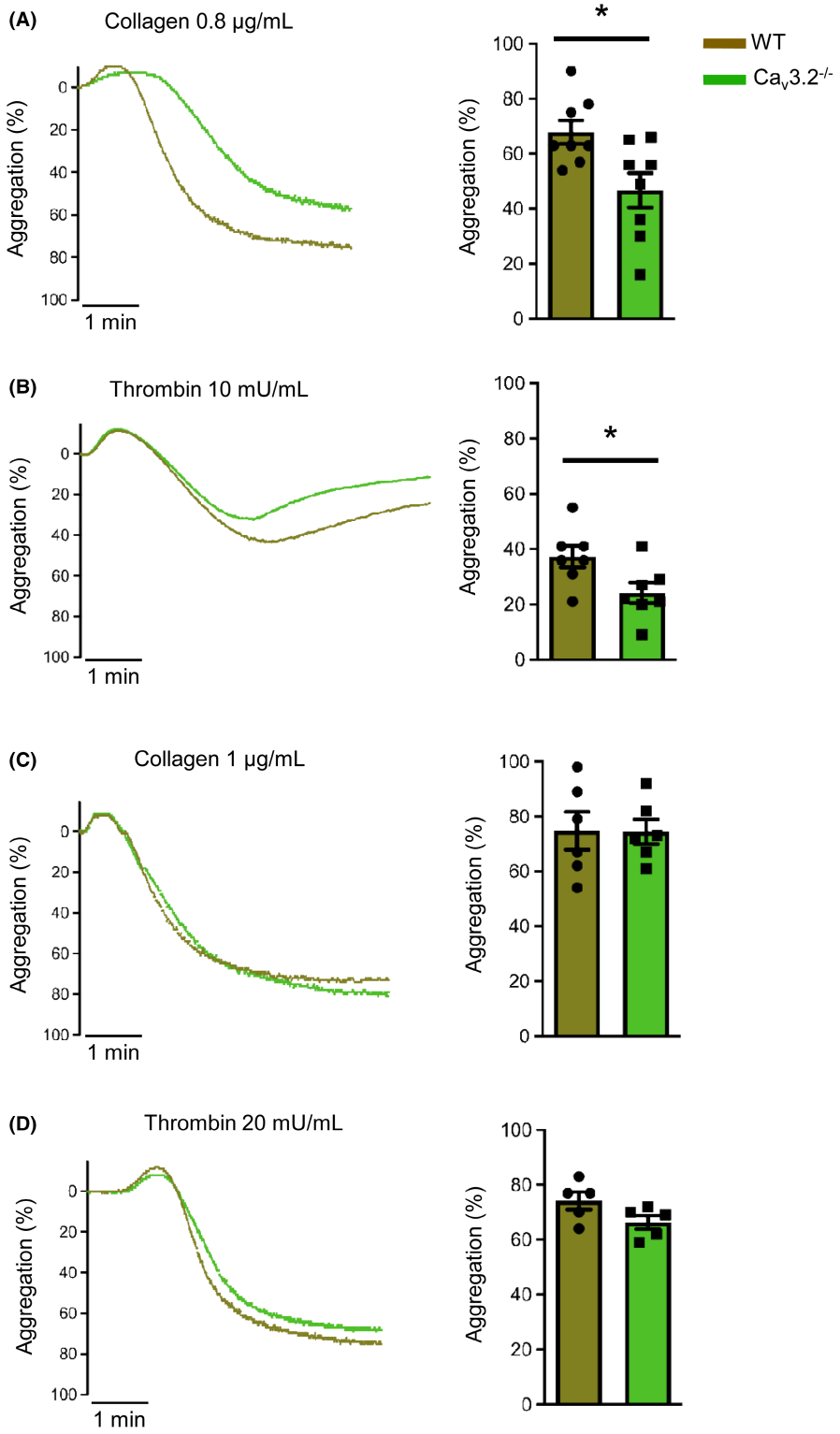

FIGURE 5 Collagen- and thrombin-mediated aggregation is impaired in $Ca_v3.2^{-/-}$ platelets. Aggregation of washed platelets in the presence of calcium (2 mM) using light transmission Chrono-log aggregometer. Comparison of WT and $Ca_v3.2^{-/-}$ platelets mediated by (A) collagen (0.8 μg/ml, $^*p = .03$, WT vs. $Ca_v3.2^{-/-}$) and (B) thrombin (10 mU/ml, $^*p = .04$, WT vs. $Ca_v3.2^{-/-}$) and (C) collagen 1 μg/ml and (D) thrombin 20 mU/ml. Data are mean ± SEM ($n = 3$–5) and were analyzed by unpaired *t*-test with Mann-Whitney *U* test. ANOVA, analysis of variance; WT, wild-type.

3.5 | Collagen- and thrombin-mediated aggregation is defective in $Ca_v3.2^{-/-}$ platelets

Platelet secretion is important for aggregation.[40] Importantly, released ADP amplifies activation signals, thus enhancing aggregation.[40,41] Defective platelet granule release may affect platelet aggregation. When activated with collagen, $Ca_v3.2^{-/-}$ platelets showed reduced aggregation compared with wild-type controls (0.8 μg/ml; 47 ± 6% vs. 68 ± 4, $p = .03$; Figure 5A) and thrombin (10 mU/ml; 24 ± 4% vs. 37 ± 4%; $p = .04$; Figure 5B). However, collagen 1 μg/ml (Figure 5C) or thrombin 20 mU/ml (Figure 5D), mediated similar aggregation of $Ca_v3.2^{-/-}$ and wild-type platelets.

$NiCl_2$ inhibits human platelet aggregation.[42] Ni^{2+} (30 μM) reduced mouse platelet aggregation induced by thrombin (10 mU/ml; 23 ± 2% for Ni^{2+}-treated platelets vs. 34 ± 4% for vehicle controls, $p = .03$; Figure 6A). Ni^{2+} dose-dependently inhibited platelet aggregation (Figure S5A). Aggregation induced by high thrombin (20 mU/ml) was not attenuated by Ni^{2+} (Figure 6B). Furthermore, Ni^{2+} treatment had no effect on the aggregation of $Ca_v3.2^{-/-}$ platelets (Figure S5B). Thus, $Ca_v3.2$ may be important for platelet aggregation.

3.6 | $Ca_v3.2$ T-type calcium channel regulates $FeCl_3$-induced arterial thrombosis

Next, we performed $FeCl_3$-induced arterial thrombosis assay.[43] Occlusion time was significantly increased in $Ca_v3.2^{-/-}$ (global) mice versus wild-type controls (11.93 ± 1.5 min vs. 8.88 ± 2.3 min, $p = .019$; Figure 7A,B). Defective arterial thrombosis could result from abnormal endothelium, platelets, or other cell types in $Ca_v3.2^{-/-}$ mice. Therefore, we generated platelet-specific $Ca_v3.2^{-/-}$ mice by crossbreeding platelet factor 4-cre ($pf4^{cre/+}$) with $Ca_v3.2^{fl/fl}$ mice (Figure S6). $Ca_v3.2^{plt-/-}$ mice showed significantly increased carotid artery occlusion time versus controls (15.22 ± 4.5 min vs. 10.98 ± 2.4 min, $p = .013$; Figure 7C,D). Histology of the carotid artery sections showed similar $FeCl_3$ treatments (Figure S7A,B).

Similarly, $Ca_v3.2^{-/-}$ ($p = .001$; Figure 7E,F) and $Ca_v3.2^{plt-/-}$ mice ($p = .001$; Figure 7G,H) showed significantly reduced thrombus growth on collagen-coated surfaces in a microfluidic chamber. Both *in vivo* and *ex vivo* results highlight the role of $Ca_v3.2$ in thrombosis. The tail bleeding time was similar between the $Ca_v3.2^{-/-}$ and wild-type mice and $Ca_v3.2^{plt-/-}$ mice and controls (146.4 ± 32.94 sec for $Ca_v3.2^{-/-}$, $n = 10$ vs. sec for 159.53 ± 23.6 WT, $n = 13$; $p = .87$; Figure S8A, and 136.5 ± 26.86 sec for $Cav3.2^{plt-/-}$,$n = 12$ vs. 166.9 ± 23.95 sec for $Ca_v3.2^{fl/fl}$, $n = 15$; $p = .31$; Figure S8B), which indicates normal hemostasis.

4 | DISCUSSION

In the current study, we found that $Ca_v3.2$ is expressed in platelets and regulates platelet $[Ca^{2+}]_i$ content. $Ca_v3.2^{-/-}$ and Ni^{2+}-treated platelets showed reduced calcium influx independent of released

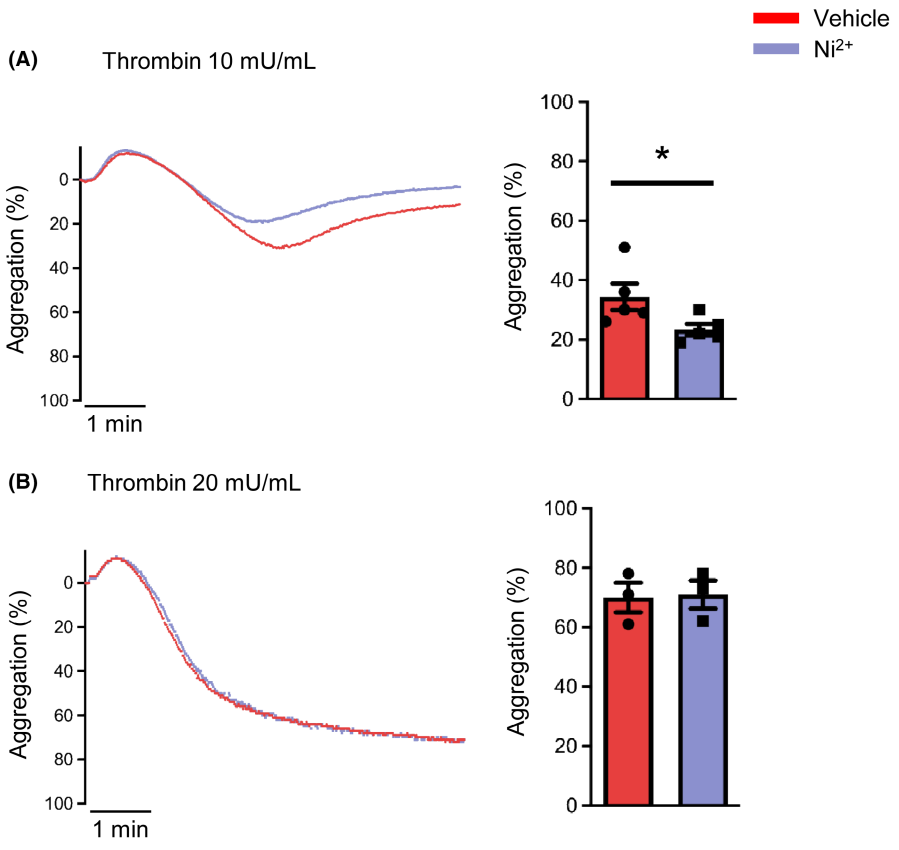

FIGURE 6 T-type calcium channel inhibitor Ni^{2+} causes decreased aggregation of platelets. (A, B) Washed platelets in the presence of vehicle (control) or Ni^{2+} (30 μM) were activated with thrombin, and aggregation was studied by aggregometry. (A) Aggregation mediated by thrombin (10 mU/ml) in Ni^{2+}-treated platelets (*$p = .03$, vehicle vs. Ni^{2+}). (B) Ni^{2+}-treated platelets showed similar aggregation as controls when activated by thrombin (20 mU/ml). Data are mean ± SEM ($n = 3$–5) and were analyzed by unpaired *t*-test with Mann-Whitney *U* test.

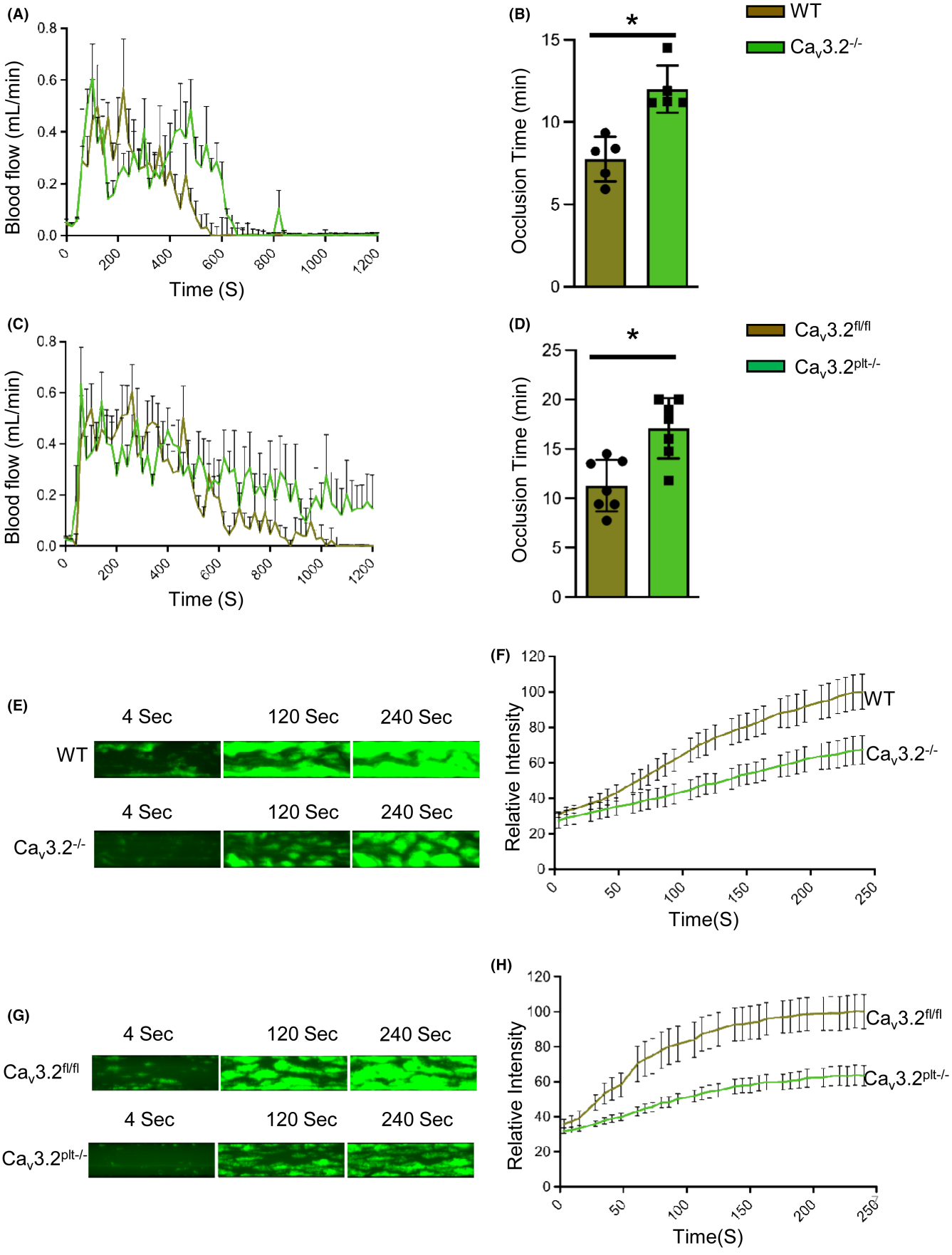
(A)
Blood flow (mL/min)
Time (S)
(B)
WT
Cav3.2-/-
Occlusion Time (min)
*
(C)
Blood flow (mL/min)
Time (S)
(D)
Cav3.2fl/fl
Cav3.2plt-/-
Occlusion Time (min)
*
(E)
4 Sec
120 Sec
240 Sec
WT
Cav3.2-/-
(F)
Relative Intensity
Time(S)
WT
Cav3.2-/-
(G)
Cav3.2fl/fl
Cav3.2plt-/-
(H)
Relative Intensity
Time(S)
Cav3.2fl/fl
Cav3.2plt-/-

FIGURE 7 Global or platelet-specific deletion of $Ca_v3.2$ leads to reduced thrombus formation. (A, C) Blood flow measurement after $FeCl_3$-induced injury of the carotid artery (WT vs. $Ca_v3.2^{-/-}$, $n = 5$ and $Ca_v3.2^{fl/fl}$ vs. $Ca_v3.2^{plt-/-}$, $n = 7$). (B, D) Quantification of occlusion time. Data are mean ± SEM and were analyzed by Student *t*-test ($n = 5$, $^*p = .02$, WT vs. $Ca_v3.2^{-/-}$; $n = 7$, $^*p = .01$, $Ca_v3.2^{fl/fl}$ vs. $Ca_v3.2^{plt-/-}$). (E, G) *Ex vivo* thrombosis on a collagen-coated surface. Green fluorescence represents the thrombus formed at the indicated times (WT vs. $Ca_v3.2^{-/-}$, $n = 10$ and $Ca_v3.2^{fl/fl}$ vs. $Cav3.2^{plt-/-}$, $n = 5$). (F, H) Quantification of thrombus growth. Data are mean fluorescence intensity ± SEM and were analyzed by one-way ANOVA repeated measures with a Holm-Sidak post-hoc test, ($n = 10$, $^*p = .001$, WT vs. $Ca_v3.2^{-/-}$; $n = 5$, $^*p = .001$, $Cav3.2^{fl/fl}$ vs. $Ca_v3.2^{plt-/-}$). ANOVA, analysis of variance; WT, wild-type.

ATP/ADP. Defects in SOCE may result in decreased calcium influx.[9,44] However, thapsigargin-mediated calcium entry via SOCE, primarily Orai1, was intact in $Ca_v3.2^{-/-}$ platelets. Unlike Orai1[45] and ligand-activated P2X1,[36] the activation and inactivation of $Ca_v3.2$ is voltage dependent.[15,46] Overlapping of activation and inactivation curves allows for calcium influx known as a "window current" through T-type calcium channels that are open at the resting membrane potential.[47] Such window currents regulate calcium-sensitive processes in nonexcitable cells such as vascular endothelial cells[47] and cortical cells of the adrenal cortex.[18] T-type calcium channels allow calcium influx in slightly depolarized nonexcitable cells.[18] Platelet membrane potential at rest is −60 mV,[44] suitable for the window current,[18,47] and agonist-mediated changes in platelet membrane potential may allow calcium entry through $Ca_v3.2$. Studies suggest that changes in membrane potential regulate calcium entry.[44,48,49] Moreover, thrombin and collagen mediate calcium entry through T-type calcium channels in pulmonary microvascular endothelial cells and smooth muscle cells.[50,51] However, further studies are required to gain insights into how calcium entry through $Ca_v3.2$ occurs in platelets.

Calcium mediates granule release and integrin activation through pERK,[32,37,52] which is significantly reduced in $Ca_v3.2^{-/-}$ and Ni^{2+}-treated platelets. This finding agrees with the previously reported $Ca_v3.2$-dependent ERK activation.[38] Next, we assessed the platelet activation by measuring platelet secretion and $\alpha_{IIb}\beta3$ activation. Although the calcium is severely reduced in SOCE-ablated platelets, activation is normal in response to thrombin.[45,53] In contrast, $Ca_v3.2^{-/-}$ and Ni^{2+}-treated platelets showed reduced platelet activation. Unlike SOCE, $Ca_v3.2$ is associated with SNARE proteins[54] and expressed near secretory vesicles.[55] Moreover, $Ca_v3.2$ regulates exocytosis in rat chromaffin cells, which is sensitive to Ni^{2+}.[22,23] A small calcium surge through $Ca_v3.2$ may be sufficient to induce platelet secretion. Therefore, platelet activation defect is evident in $Ca_v3.2^{-/-}$ but not in SOCE ablated platelets.[45,53] The paracrine activity of the released ATP/ADP induces activation amplification and aggregation. Therefore, we assessed platelet aggregation. As expected, $Ca_v3.2^{-/-}$ and Ni^{2+}-treated platelets showed decreased aggregation.

Next, we performed both *in vivo* and *ex vivo* thrombosis assays. $Ca_v3.2$ deletion (global or platelet-specific) decreased arterial thrombosis and thrombus growth on a collagen-coated surface. Increased occlusion time in the absence of $Ca_v3.2$ may be due to increased embolism. Decreased thrombus growth on a collagen-coated surface indicates the possibility of embolization. However, a study of emboli formation is required to support our hypothesis. However, our tail bleeding assay indicated normal hemostasis in $Ca_v3.2^{-/-}$ mice. This discrepancy could be due to differences in injury type, site of injury, the blood vessels involved, blood flow rates, and injury-dependent activation of various pathways of the coagulation cascade.

The limitation of our study is the lack of mechanisms of $Ca_v3.2$-mediated exocytosis. However, there could be two possible mechanisms. First, the interaction of $Ca_v3.2$ with SNARE proteins governs low-threshold exocytosis, as observed in chromaffin cells.[55] Both platelets and chromaffin cells share similar exocytosis mechanisms mediated by calcium influx, which could be an explanation.[56] Future studies are required to unveil such association. Second, calcium influx can mediate granule exocytosis via ERK activation.[32]

Hypertensive and diabetic patients are at risk of cardiovascular complications and kidney disease.[57–59] Aspirin has been the drug of choice to prevent cardiovascular complications[58] but causes bleeding and stroke.[60] Some patients are also intolerant to aspirin,[58] which highlights the need for an efficient and safe antiplatelet drug. Efonidipine can improve vascular endothelial function[14] via its role in T-type calcium channels and also has antiplatelet activity.[10] Additionally, T-type calcium channel blockers have a protective effect on renal function.[61,62] Our findings indicate that the development of drugs targeting $Ca_v3.2$ may help lessen the risk of cardiovascular complications.

ACKNOWLEDGMENTS

The authors thank the Pathology Core and the Flow Cytometry Core facilities at the Institute of Biomedical Sciences, Academia Sinica, Taiwan (AS-CFII108-113). They thank the Taiwan Mouse Clinic, Academia Sinica, and Taiwan Animal Consortium for technical support in performing complete blood count and the Transgenic Mouse Model Core at the National Core Facility for Biopharmaceuticals, Ministry of Science and Technology (MOST), Taiwan.

CONFLICT OF INTEREST

None declared.

AUTHOR CONTRIBUTIONS

H.K.T., B.H.T., and C.C.C. conceived the idea for the study, designed the research, and wrote the manuscript. H.K.T. performed the experiments, collected and analyzed the data, and wrote the manuscript. S.C.H. generated the floxed mice. B.H.T. designed and performed the experiments. R.B.Y. and Y.C.T. designed the experiments. Z.H.S. performed the experiments. C.C.P performed the experiments. All authors edited and reviewed the final version of the manuscript.

ORCID

Hem Kumar Tamang https://orcid.org/0000-0003-2377-751X
Ruey-Bing Yang https://orcid.org/0000-0003-3017-3714
Zong-Han Song https://orcid.org/0000-0003-2169-4796
Shao-Chun Hsu https://orcid.org/0000-0002-6995-9338
Chien-Chung Peng https://orcid.org/0000-0002-1458-5287
Yi-Chung Tung https://orcid.org/0000-0002-6170-2992
Bing-Hsiean Tzeng https://orcid.org/0000-0002-4767-9570
Chien-Chang Chen https://orcid.org/0000-0001-8850-4278

REFERENCES

1. Costa MA, Simon DI. Molecular basis of restenosis and drug-eluting stents. *Circulation*. 2005;111:2257-2273.
2. Davis C, Fischer J, Ley K, Sarembock IJ. The role of inflammation in vascular injury and repair. *J Thromb Haemost*. 2003;1:1699-1709.
3. Forrester JS, Fishbein M, Helfant R, Fagin J. A paradigm for restenosis based on cell biology: clues for the development of new preventive therapies. *J Am Coll Cardiol*. 1991;17:758-769.
4. Gawaz M, Langer H, May AE. Platelets in inflammation and atherogenesis. *J Clin Invest*. 2005;115:3378-3384.
5. Orford JL, Selwyn AP, Ganz P, Popma JJ, Rogers C. The comparative pathobiology of atherosclerosis and restenosis. *Am J Cardiol*. 2000;86:6H-11H.
6. Davì G, Patrono C. Platelet activation and atherothrombosis. *N Engl J Med*. 2007;357:2482-2494.
7. Furie B, Furie BC. Mechanisms of thrombus formation. *N Engl J Med*. 2008;359:938-949.
8. Gibbins JM. Platelet adhesion signalling and the regulation of thrombus formation. *J Cell Sci*. 2004;117:3415-3425.
9. Varga-Szabo D, Braun A, Nieswandt B. Calcium signaling in platelets. *J Thromb Haemost*. 2009;7:1057-1066.
10. Nomura S, Kanazawa S, Fukuhara S. Effects of efonidipine on platelet and monocyte activation markers in hypertensive patients with and without type 2 diabetes mellitus. *J Hum Hypertens*. 2002;16:539-547.
11. Harper MT, Poole AW. Store-operated calcium entry and non-capacitative calcium entry have distinct roles in thrombin-induced calcium signalling in human platelets. *Cell Calcium*. 2011;50:351-358.
12. Gilio K, van Kruchten RV, Braun A, et al. Roles of platelet STIM1 and orai1 in glycoprotein VI- and thrombin-dependent procoagulant activity and thrombus formation. *J Biol Chem*. 2010;285(31):23629-23638.
13. Nesbitt WS, Kulkarni S, Giuliano S, et al. Distinct glycoprotein Ib/V/IX and integrin aIIb3-dependent calcium signals cooperatively regulate platelet adhesion under flow. *J Biol Chem*. 2002;277(4):2965-2972.
14. Oshima T, Ozono R, Yano Y, et al. Beneficial effect of T-type calcium channel blockers on endothelial function in patients with essential hypertension. *Hypertens Res*. 2005;28:889-894.
15. Powell KL, Cain SM, Snutch TP, O'Brien TJ. Low threshold T-type calcium channels as targets for novel epilepsy treatments. *Br J Clin Pharmacol*. 2014;77:729-739.
16. Cribbs LL. Vascular smooth muscle calcium channels: could "T" be a target? *Circ Res*. 2001;89:560-562.
17. Bernal Sierra YA, Haseleu J, Kozlenkov A, Bégay V, Lewin GR. Genetic tracing of Cav3.2 T-type calcium channel expression in the peripheral nervous system. *Front Mol Neurosci*. 2017;10(70):1-17.
18. Rossier MF. T-Type calcium channel: a privileged gate for calcium entry and control of adrenal steroidogenesis. *Front Endocrinol*. 2016;7(43):1-17.
19. Wang H, Zhang X, Xue L, et al. Low-voltage-activated CaV3.1 calcium channels shape T helper cell cytokine profiles. *Immunity*. 2016;44(4):782-794.
20. Zhou C, Chen H, King JA, et al. α1G T-type calcium channel selectively regulates P-selectin surface expression in pulmonary capillary endothelium. *Am J Physiol Lung Cell Mol Physiol*. 2010;299:L86-L97.
21. Cove-Smith A, Mulgrew CJ, Rudyk O, et al. Anti-proliferative actions of T-type calcium channel inhibition in Thy1 nephritis. *Am J Pathol*. 2013;183:391-401.
22. Giancippoli A, Novara M, de Luca A, et al. Low-threshold exocytosis induced by cAMP-recruited CaV3.2 (alpha1H) channels in rat chromaffin cells. *Biophys J*. 2006;90(5):1830-1841.
23. Carabelli V, Marcantoni A, Comunanza V, et al. Chronic hypoxia up-regulates α_{1H}T-type channels and low threshold catecolamine secretion in rat chromaffin cells. *J Physiol*. 2007;584:149-165.
24. Chiang C-S, Huang C-H, Chieng H, et al. The $Ca_V3.2$ T-type Ca^{2+} channel is required for pressure overload–induced cardiac hypertrophy in mice. *Circ Res*. 2009;104:522-530.
25. Lin S-S, Tzeng B-H, Lee K-R, Smith RJH, Campbell KP, Chen CC. $Ca_v3.2$ T-type calcium channel is required for the NFAT-dependent Sox9 expression in tracheal cartilage. *PNAS*. 2014;111(19):E1990-E1998.
26. Tzeng B-H, Chen Y-H, Huang C-H, Lin S-S, Lee K-R, Chen C-C. The $Ca_v3.1$ T-type calcium channel is required for neointimal formation in response to vascular injury in mice. *Cardiovasc Res*. 2012;96:533-542.
27. Zhou C, Chen H, Lu F, et al. $Ca_v3.1$ (α_{1G}) controls von Willebrand factor secretion in rat pulmonary microvascular endothelial cells. *Am J Physiol Lung Cell Mol Physiol*. 2007;292:L833-L844.
28. Chen C-C, Lamping KG, Nuno DW, et al. Abnormal coronary function in mice deficient in α_{1H} T-type Ca^{2+} channels. *Science*. 2003;302:1416-1418.
29. Tiedt R, Schomber T, Hao-Shen H, Skoda RC. Pf4-Cre transgenic mice allow the generation of lineage-restricted gene knockouts for studying megakaryocyte and platelet function in vivo. *Blood*. 2007;109:1503-1506.
30. Tsai H-J, Huang C-L, Chang Y-W, et al. Disabled-2 is required for efficient hemostasis and platelet activation by thrombin in mice. *Arterioscler Thromb Vasc Biol*. 2014;34(11):2404-2412.
31. Ohlmann P, Hechler B, Cazenave J-P, Gachet C. Measurement and manipulation of $[Ca^{2+}]_i$ in suspensions of platelets and cell cultures. *Methods Mol Biol*. 2004;273:229-240.
32. Stefanini L, Roden RC, Bergmeier W. CalDAG-GEFI is at the nexus of calcium-dependent platelet activation. *Blood*. 2009;114:2506-2514.
33. Konopatskaya O, Gilio K, Harper MT, et al. PKCα regulates platelet granule secretion and thrombus formation in mice. *J Clin Invest*. 2009;119:399-407.
34. Todorovic SM, Lingle CJ. Pharmacological properties of T-type Ca^{2+} current in adult rat sensory neurons: effects of anticonvulsant and anesthetic agents. *J Neurophysiol*. 1998;79:240-252.
35. Kang H-W, Park J-Y, Jeong S-W, et al. A molecular determinant of nickel inhibition in $Ca_v3.2$ T-type calcium channels. *J Biol*. 2006;281:4823-4830.
36. Toth-Zsamboki E, Oury C, Cornelissen H, De Vos R, Vermylen J, Hoylaerts MF. P2X1-mediated ERK2 activation amplifies the collagen-induced platelet secretion by enhancing myosin light chain kinase activation. *J Biol Chem*. 2003;278:46661-46667.
37. Nadal-Wollbold F, Pawlowski M, Levy-Toledano S, Berrou E, Rosa JP, Bryckaert M. Platelet ERK2 activation by thrombin is dependent on calcium and conventional protein kinases C but not Raf-1 or B-Raf. *FEBS Lett*. 2002;531:475-482.
38. Chen W-K, Liu I-Y, Chang Y-T, et al. $Ca_v3.2$ T-Type Ca^{2+} channel-dependent activation of ERK in paraventricular thalamus modulates acid-induced chronic muscle pain. *J Neurosci*. 2010;30(10):10360-10368.

39. Bye AP, Gibbins JM, Mahaut-Smith MP. Ca^{2+} waves coordinate purinergic receptor–evoked integrin activation and polarization. *Sci Signal*. 2020;13(615):1-12.
40. Estevez B, Du X. New concepts and mechanisms of platelet activation signaling. *Physiology*. 2017;32:162-177.
41. Ohlmann P, Eckly A, Freund M, Cazenave JP, Offermanns S, Gachet C. ADP induces partial platelet aggregation without shape change and potentiates collagen-induced aggregation in the absence of Gαq. *Blood*. 2000;96:2134-2139.
42. Chen CY, Lin TH. Effects of nickel chloride on human platelets: enhancement of lipid peroxidation, inhibition of aggregation and interaction with ascorbic acid. *J Toxicol Environ Health A*. 2001;62:431-438.
43. Eckly A, Hechler B, Freund M, et al. Mechanisms underlying $FeCl_3$-induced arterial thrombosis. *J Thromb Haemost*. 2011;9:779-789.
44. MacIntyre DE, Rink TJ. The role of platelet membrane potential in the initiation of platelet aggregation. *J Thromb Haemost*. 1982;47:22-26.
45. Braun A, Varga-Szabo D, Kleinschnitz C, et al. Orai1 (CRACM1) is the platelet SOC channel and essential for pathological thrombus formation. *Blood*. 2009;113:2056-2063.
46. Kim J-A, Park J-Y, Kang H-W, Huh S-U, Jeong S-W, Lee J. Augmentation of $Ca_v3.2$ T-type calcium channel activity by cAMP-dependent protein kinase A. *JPET*. 2006;318:230-237.
47. Senatore A, Zhorov BS, Spafford JD. Cav3 T-type calcium channels. *WIREs Membr Transp Signal*. 2012;1:467-491.
48. Harper MT, Poole AW. Chloride channels are necessary for full platelet phosphatidylserine exposure and procoagulant activity. *Cell Death Dis*. 2013;4:e969.
49. Kovács T, Tordai A, Szász I, Sarkadi B, Gárdos G. Membrane depolarization inhibits thrombin-induced calcium influx and aggregation in human platelets. *FEBS*. 1990;266:171-174.
50. Wu S, Haynes J, Taylor JT, et al. $Ca_v3.1$ (α1G) T-Type Ca^{2+} channels mediate vaso-occlusion of sickled erythrocytes in lung microcirculation. *Circ Res*. 2003;93:346-353.
51. Hénaff M, Quignard JF, Biendon N, Morel JL, Macrez N. T-type calcium channels involved in collagen fragment-induced smooth muscle cell death. *Calcium Signal*. 2014;1:15-23.
52. Oury C, Toth-Zsamboki E, Vermylen J, Hoylaerts MF. P2X1-mediated activation of extracellular signal-regulated kinase 2 contributes to platelet secretion and aggregation induced by collagen. *Blood*. 2002;100:2499-2505.
53. Varga-Szabo D, Braun A, Kleinschnitz C, et al. The calcium sensor STIM1 is an essential mediator of arterial thrombosis and ischemic brain infarction. *J Exp Med*. 2008;205:1583-1591.
54. Weiss N, Hameed S, Fernandez-Fernandez JM, et al. $Ca_v3.2$/Syntaxin-1A signaling complex controls T-type channel activity and low-threshold exocytosis. *J Biol Chem*. 2012;287:2810-2818.
55. Mahapatra S, Calorio C, Vandael DHF, Marcantoni A, Carabelli V, Carbone E. Calcium channel types contributing to chromaffin cell excitability, exocytosis and endocytosis. *Cell Calcium*. 2012;51:321-330.
56. Fitch-Tewfik JL, Flaumenhaft R. Platelet granule exocytosis: a comparison with chromaffin cells. *Endocrinol*. 2013;4:77.
57. Ferroni P, Basili S, Falco A, Davì G. Platelet activation in type 2 diabetes mellitus. *J Thromb Haemost*. 2004;2:1282-1291.
58. Blann AD, Nadar S, Lip GYH. Pharmacological modulation of platelet function in hypertension. *Hypertension*. 2003;42:1-7.
59. Duan J, Wang C, Liu D, et al. Prevalence and risk factors of chronic kidney disease and diabetic kidney disease in Chinese rural residents: a cross-sectional survey. *Sci Rep*. 2019;9:10408.
60. Bautista LE, Vera LM. Antihypertensive effects of aspirin: what is the evidence? *Curr Hypertens Rep*. 2010;12:282-289.
61. Thamcharoen N, Susantitaphong P, Wongrakpanich S, et al. Effect of N- and T-type calcium channel blocker on proteinuria, blood pressure and kidney function in hypertensive patients: a meta-analysis. *Hypertens Res*. 2015;38:847-855.
62. Li X, Yang MS. Effects of T-type calcium channel blockers on renal function and aldosterone in patients with hypertension: a systematic review and meta-analysis. *PLoS One*. 2014;9:e109834.

SUPPORTING INFORMATION

Additional supporting information may be found in the online version of the article at the publisher's website.

How to cite this article: Tamang HK, Yang R-B, Song Z-H, et al. $Ca_v3.2$ T-type calcium channel regulates mouse platelet activation and arterial thrombosis. *J Thromb Haemost*. 2022;20:1887–1899. doi:10.1111/jth.15745